Improved Optoelectronic Characteristics of Light-Emitting Diodes by Using a Dehydrated Nanotube Titanic Acid (DNTA)−Polymer Nanocomposite

L. Qian,*,† F. Teng,† Z.-S. Jin,‡ Z.-J. Zhang,‡ T. Zhang,† Y.-B. Hou,† S.-Y. Yang,† and X.-R. Xu†

Institute of Optoelectronics, Beijing Jiaotong University, Beijing 100044, China, and Key Laboratory on Special Functional Materials, Henan University, Kaifeng 475001, China

Received: June 4, 2004; In Final Form: July 16, 2004

In this paper, we have demonstrated that P-type dehydrated nanotube titanic acid (DNTA) can significantly enhance hole injection and transport in holes-only transport devices. In the low field region, the dominant conduction mechanism is injection limited. This gradually transitions to space charge limited current via trapped charge limited current with increasing applied voltages. Through fabricated and characterized organic light-emitting diodes (OLEDs) and by using a DNTA−poly(vinylcarbazole) (PVK) nanocomposite as the hole transport layer, we found that the performance of these devices was greatly improved with a higher luminance, an enhanced efficiency, and a lower turn-on voltage.

I. Introduction

With the microminiaturization of optoelectronic devices, more novelty low-dimension nanomaterials are required. Since being founded by Iijima in 1991,[1] the carbon nanotube has attracted tremendous interest from researchers in different fields because one-dimension nanomaterials have extensive potential applications in nanodevices and middlecosmic systems. By now, nanotubes, nanorods, and nanowires have been made from different materials.[2−7] The incorporation of one-dimension nanomaterials into the conducting polymers has been considered as an efficient scheme for improving the carriers' transport ability and the luminescence efficiency of the device in recent years.[8−11] Single-walled carbon nanotubes (SWNTs) as a promising candidate for a composite component have been investigated extensively.[12−14] Due to their good electron-transporting property, SWNTs have been doped into conductive polymers to increase electron mobility and luminescence efficiency, but the electroluminescence (EL) intensity of LEDs decreased significantly when SWNTs were doped into a hole-conducting buffer layer (PEDOT:PSS) as the result of the hole-blocking effect.

In this paper, the morphology and electric properties of dehydrated nanotube titanic acid (DNTA) were characterized. When P-type DNTA was doped into poly(vinylcarbazole) (PVK), the hole injection and transport of holes-only devices (ITO/PVK:DNTA/Al) improved significantly, as compared with those devices without DNTA. The organic light-emitting diodes (OLEDs) in which a DNTA−polymer composite functions as the hole transport layer show an enhanced efficiency with a higher luminance and a lower turn-on voltage.

II. Experimental Section

2.1. Synthesis of DNTA. The DNTA, in our experiments, was synthesized by the wet method.[15−16] A 120 mL portion of NaOH aqueous solution (40 wt %) was placed in a PTFE bottle equipped with a reflux condenser. Then, the bottle was placed in an oil bath, where the solution was heated to 110 °C; 2 g of TiO_2 (anatase) (Degussa P-25) was added to the above solution and refluxed with magnetic stirring for 20 h. After the reaction stopped and cooled to room temperature, the solid was separated out and neutralized with 0.1 M HCl solution to pH ∼ 5, filtered, and washed with distilled water until free from Cl^-. The solid product was dried under vacuum at room temperature to yield DNTA.

Figure 1 shows the transmission electron microscopic (TEM) images of TiO_2 (anatase) P-25 and DNTA. The inner and outer diameters of DNTA are equal to ∼6.4 and ∼9.3 nm, respectively, and the distance between adjacent layers is ∼0.8 nm. The length of DNTA is ∼100 nm. After being annealed at 500 °C in air for 5 h, the structure of DNTA was not destroyed, which demonstrated DNTA has good thermal stability.

2.2. Electric Characteristics of DNTA. DNTA film was deposited on an ITO electrode in a 0.1 M solution of $NaSO_4$ with platinum as a counter electrode. Figure 2 shows the photocurrent against applied voltage from the DNTA layer was observed with a visible light illumination of 0.7 mW/cm^2 (λ_{inc} > 420 nm). It was found that the open circuit voltage (U_{oc}) and short circuit current (I_{sc}) were 4 mV and 0.006 μA, respectively. Obviously, the P-type conductivity of DNTA can be seen from the photocurrent curve.

To investigate the improvement of hole transport by doping DNTA into poly(vinylcarbazole) (PVK), the holes-only devices were fabricated, which are denoted as A_0 for undoped PVK, A_1 for 1 wt % DNTA in PVK, A_2 for 2 wt % DNTA in PVK, and A_5 for 5 wt % DNTA in PVK, respectively. The thickness of the PVK layer in all these devices is ∼120 nm. In PVK composite devices, the current−voltage characteristics are measured. The overall characteristics show three different regimes, and each can be fitted with the power law $J \propto V^{l+1}$, with l varying from $l < 2$ at low V to 4.5−8 at intermediate V to ∼2 at high V, respectively (Figure 3a). The first evolution corresponds to the transition from injection limited conduction to trapped charge limited (TCL) conduction rather than from

* Corresponding author. Phone: 86-010-51684908. Fax: 86-010-51688018. E-mail: qian_lei@126.com.
† Beijing Jiaotong University.
‡ Henan University.

10.1021/jp047593a CCC: $27.50
Published on Web 08/24/2004

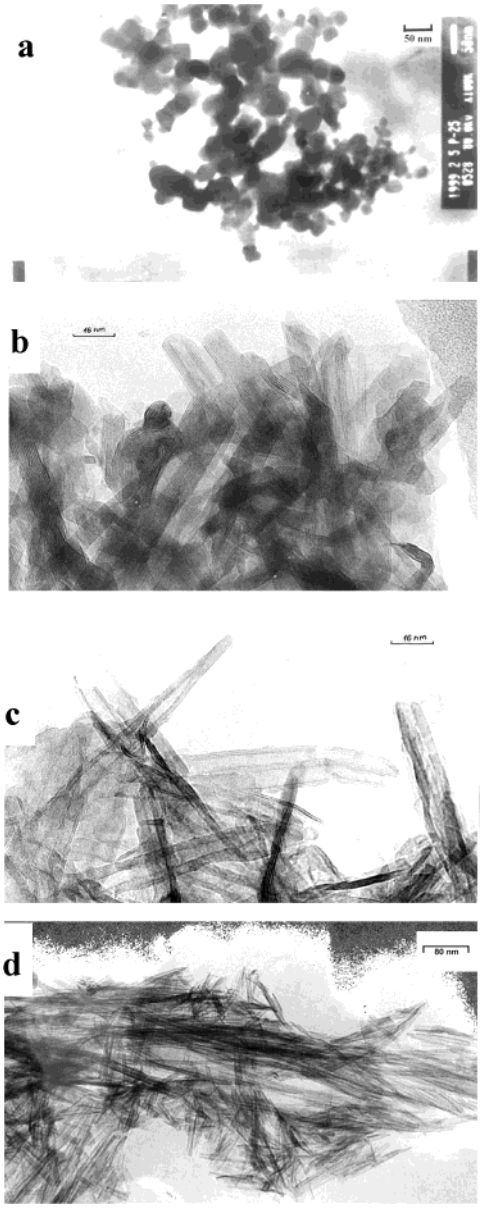

Figure 1. Transmission electron microscopic (TEM) images of TiO_2 (anatase) P-25 and DNTA: (a) P-25 ($\times 10^5$); (b) DNTA after being annealed in air at 500 °C for 5 h ($\times 1.25 \times 10^6$); (c) DNTA as prepared ($\times 1.25 \times 10^6$); (d) DNTA as prepared ($\times 2.5 \times 10^5$).

ohmic conduction to trapped charge limited conduction, due to this transition voltage kept at ~10 V with different PVK layer thicknesses (as shown in Figure 3b).[17] The occurrence of trapped charge limited and space charge limited current requires that at least one contact has good injecting properties to provide an inexhaustible carrier reservoir, but in this case, the injection barriers for both carriers were quite large. The transition voltage was ~5 V for A_5 and ~10 V for A_0, which implied reduction of the hole injection barrier due to the addition of DNTA into the PVK layer. In the TCL region, the value of $l = E_t/kT$ is ~8 for A_0 and ~4.5 for A_5. The parameter E_t is directly related to the steepness and depth of the exponential trap distribution. A smaller value of E_t indicates that there is a much steeper distribution closer to the valence band.[18] The trap depth for A_5 is ~0.11 eV compared to ~0.20 eV for A_0. This implied that there was interaction between DNTA and PVK, which changed the depth and density of traps in the PVK layer and induced more rigidization of the polymer chains to facile hole transport. The hole capture probability of a trap is given by $f_p(E) = 1/\{1$

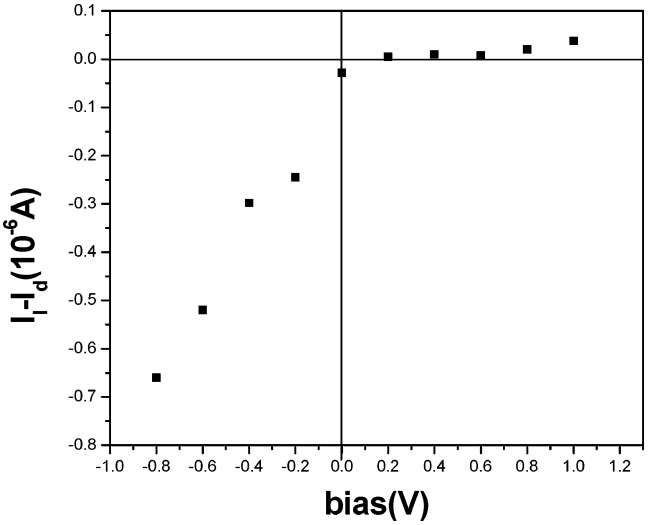

Figure 2. Photocurrent−potential spectrum of DNTA (I_l, current under illumination; I_d, current under dark).

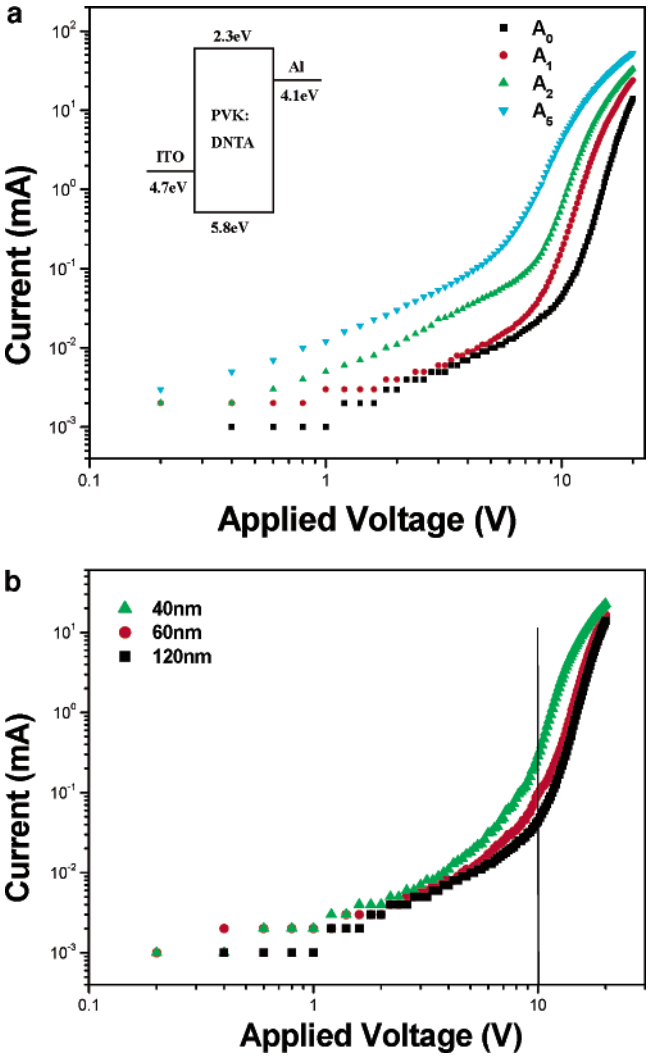

Figure 3. (a) The energy diagram (inset) and current−voltage characteristics for devices A_0−A_5. (b) Current−voltage characteristics of device A_0 at different PVK thicknesses.

$+ g_p \exp[(E_{F_p} - E_t)/kT]\}$,[19] where g_p is the united density of trap states and $E_{F_p} - E_t$ is the gap between the trap level and the valence band. The hole traps were filled faster as the value of $E_{F_p} - E_t$ increased, so the slope of the $I-V$ curve for A_0 is steeper than that for A_5. When the hole traps were fully filled

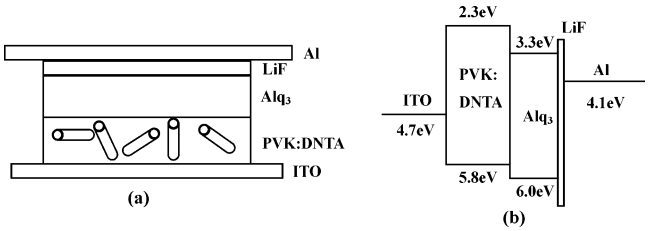

Figure 4. Schematic diagrams of (a) the device structure and (b) the energy band of these OLEDs.

with increasing applied voltage, the $I-V$ characteristics exhibit space charge limited current with free traps. It is found that the voltage of the second transition, that is, current due to trapped charge limited to space charge limited with free trap, increased with increasing layer thickness and the number of traps. For example, it decreased from ~20 V for A_0 to ~12 V for A_5. This indicated an improvement in charge transport for doped PVK devices. The effective hole carrier mobility (μ_{eff}) can be determined from the region with $m = 2$ through the Child equation: $\mu_{eff} = (8/9\epsilon)J_{SCL}(d^3/V^2)$,[10] where ϵ is the dielectric constant ($\epsilon = 3$ for PVK), J_{SCL} is the current density, d is the thickness of the device, and V is the applied voltage. The best fit to the data shows that the mobility of A_0 is estimated to be ~1.42×10^{-7} cm^2 V^{-1} s^{-1} and μ_{eff} reaches up to 5.38×10^{-7} cm^2 V^{-1} s^{-1} for A_5. The mobility obtained from the nanotube-free devices shows good agreement with the previously known value 1.4×10^{-7} cm^2 V^{-1} s^{-1} measured using the time-of-flight method.[20]

2.3. Fabrication and Characteristics of Light-Emitting Diodes. The undoped poly(vinylcarbazole) (PVK) and doped ones with 1, 2, and 5 wt % DNTA into PVK in chloroform solution were spin-coated on cleaned ITO-coated glass substrate. The thickness of the composite films is ~120 nm. Alq_3 (120 nm) was deposited onto the nanocomposite layer by the thermal evaporation method as the electron transport and emitting layer. Then, a bilayer cathode of LiF (1 nm)−Al (200 nm) was used as the top electrode. The devices with different doped proportions of DNTA were denoted as D_0 for undoped PVK, D_1 for 1 wt % DNTA doped PVK, D_2 for 2 wt % DNTA doped PVK, and D_5 for 5 wt % DNTA doped PVK, respectively. A summary of the device structures and energy band diagrams in this work is shown in Figure 4.

In Figure 5, luminance−voltage and current−voltage characteristics of the devices are shown. The maximum luminance of D_2 is ~1 order of magnitude higher than that of D_0. The turn-on voltages decreased from 12 V for D_0 to 8 V for D_2. Significantly lower turn-on and operating voltages are achieved in the composites due to the reduction barrier for the injection of holes from the ITO anode to DNTA. However, if the mass fraction of DNTA in PVK is too high, the performance and stability of devices made from it will degrade because the structure and configuration of PVK films had been destroyed, even though the current density increased with the dopant ratio.

Obviously, the device current increased with the doped fraction of DNTA in the composite. The P-type conductive property of DNTA can improve the hole-transporting ability of the PVK layer. As mentioned above, DNTA can also reduce the injection barrier for holes.

Compared with D_0, it is more efficient for D_2, as the efficiency increased from 1.3 to 2.4 cd/A (1248 cd/m^2), and it gradually increases with current density. The efficiency for D_0 decreases with current density (not shown in here). The reason can be understood in this way: the injection barrier for holes is ~1.1 eV for device D_0, and it is far higher than the injection

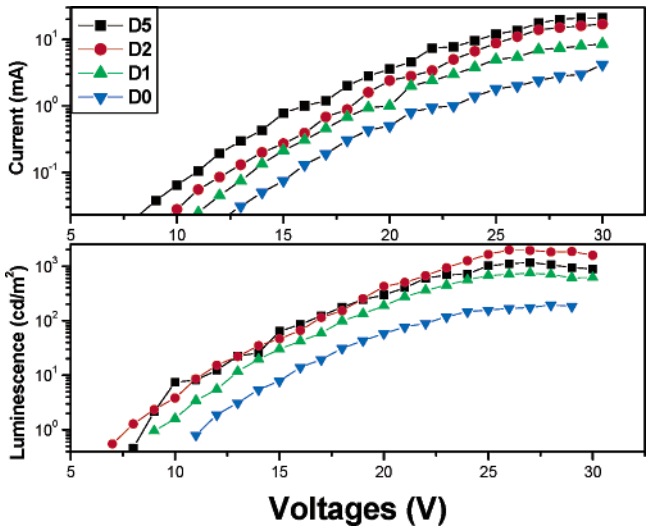

Figure 5. Current−voltage and luminance−voltage characteristics for devices D_0-D_5.

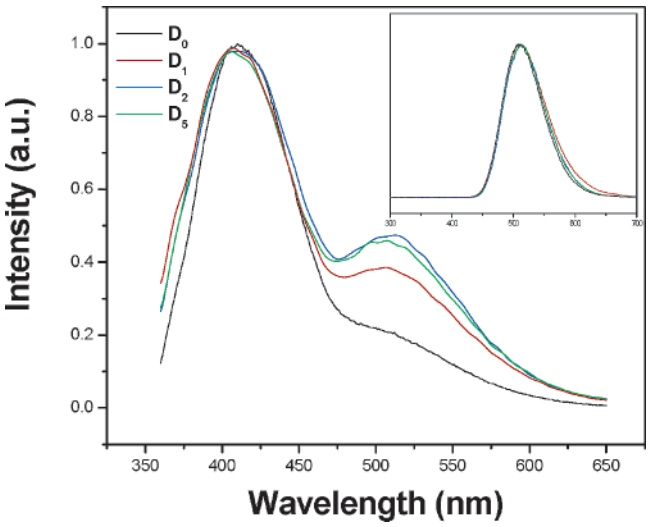

Figure 6. Normalized PL and EL spectra (inset) for devices D_0-D_5.

barrier for electrons (~0.5 eV).[21−22] The unbalance of charge carrier injection made its efficiency very low. Electron injection increases more rapidly than hole injection with an increase in the applied voltage, so its efficiency decreases with current density. For D_2, the hole injection and transport ability can be improved by doping DNTA. The balance of carrier injections can enhance device efficiency evidently. On the other hand, the improvement of the hole transport ability made the recombination region shift from the PVK/Alq_3 interface to Alq_3 bulk gradually with applied voltages. The exciton disassociation by energy mismatching and the quenching effect of Alq_3 cations at the interface was suppressed; therefore the luminescence efficiency was improved.[23] Device efficiency decreased dramatically due to the thermal-induced quenching effect under high current density. Since the recombination region closes to metal electrodes, the strong quenching effect of the Al cathode to luminescence is also an important reason for its decreased efficiency.

The typical normalized photoluminescence (PL) and electroluminescence (EL) spectra of these OLEDs are shown in Figure 6. The PL spectra demonstrate that there must be some interactions between polymer and DNTA, in which PVK molecules can combine with the defects in DNTA.[24] The composite devices show stronger emission of Alq_3 than that of

D_0, and the relative emission intensity of Alq_3 varies with different doped fractions of DNTA in PVK. These findings demonstrate that the dissociation of excitons at the PVK−DNTA nanointerface quenches PVK photoluminescence and enhances photocarrier generation and their transport between the nanocomposite layer and the Alq_3 layer. Emission only from Alq_3 can be observed in the EL spectra, which implies that the recombination occurs in the electron transport layer.

In conclusion, the carrier transport mechanisms of the holes-only device doped with DNTA have been studied. In the low field region, the carrier conduction was limited by the injection barrier. The mechanism of current conduction changed to TCL and then to SCLC in sequence with increasing the applied voltages. The effective hole mobility is enhanced and the hole barrier is reduced due to the P-type conductivity of DNTA. These OLEDs by using a DNTA−PVK nanocomposite as the hole transport layer show better performance, such as higher luminescence, enhanced efficiency, and lower turn-on voltages.

Acknowledgment. This work was supported by the NSFC (no. 90301004 and no. 10374001) and state key project of basic research MOST: 2003CB314707, China, and the Science foundation of BJTU (project no. 2003SM001).

References and Notes

(1) Iijima, S. *Nature* **1991**, *354*, 56.
(2) Tenne, R.; Margulis; Genut, M.; et al. *Nature* **1992**, *360*, 444.
(3) Chopra, N. G.; Luyken, R. J.; Cherrey, K.; et al. *Science* **1995**, *269*, 966.
(4) Zhou, D.; Seraphin, S. *Chem. Phys. Lett.* **1994**, *222*, 223.
(5) Han, W. Q.; Fan, S. S.; Li, Q. Q.; et al. *Chem. Phys. Lett.* **1997**, *265*, 374.
(6) Fasol, G.; Runge, K. *Appl. Phys. Lett.* **1997**, *70*, 2467.
(7) Morales, A. M.; Lieber, C. M. *Science* **1998**, *279*, 208.
(8) Fournet, P.; Coleman, J. N.; Lahr, B.; Drury, A.; Blau, W. J.; O'Brien, D. F.; Hörhold, H.-H. *J. Appl. Phys.* **2001**, *90*, 969.
(9) Curran, S. A.; Ajayan, P. M.; Blau, W. J.; Carroll, D. L.; Coleman, J. N.; Dalton, A. B.; Davey, A. P.; Drury, A.; McCarthy, B.; Maier, S.; Strevens, A. *Adv. Mater.* **1998**, *10*, 1091.
(10) Coleman, J. N.; Curran, S.; Holme, A. B.; Davey, A. P.; McCarthy, B.; Blau, W.; Barklie, R. C. *Phys. Rev. B* **1998**, *58*, 7492.
(11) Kim, J. Y.; Kim, M.; Choi, J. H. *Synth. Met.* **2003**, *139*, 565.
(12) Kim, J. Y.; Kim, M.; Kim, H. M.; Joo, J.; Choi, J. H. *Opt. Mater.* **2002**, *21*, 147.
(13) Woo, H. S.; Czerw, R.; Webster, S.; Carroll, D. L.; Ballato, J.; Strevens, A. E.; O'Brien, D.; Blau, W. J. *Appl. Phys. Lett.* **2000**, *77*, 1393.
(14) Woo, H. S.; Czerw, R.; Webster, S.; Carroll, D. L.; Park, J. W.; Lee, J. H. *Synth. Met.* **2001**, *116*, 369.
(15) Yang, J.; Jin, Z.; Wang, X.; Li, W.; Zhang, J.; Zhang, S.; Guo, X.; Zhang, Z. *J. Chem. Soc., Dalton Trans.* **2003**, *20*, 3898.
(16) Kasuga, T.; Hiramatsu, M.; Hoson, A.; Sekino, T.; Niihara, K. *Langmuir* **1998**, *14*, 3160.
(17) Brütting, W.; Berleb, S.; Mückl, A. G. *Org. Electron.* **2001**, *2*, 1.
(18) Brütting, W.; Berleb, S.; Mückl, A. G. *Synth. Met.* **2001**, *122*, 99.
(19) Kao, K. C.; Huang, W. *Electrical Transport in Solids*; Pergamon Press: Oxford, U.K., 1981.
(20) Williams, D. J.; Limburg, W. W.; Pearson, J. M.; Goedde, A. O.; Yanus, J. F. *J. Chem. Phys.* **1975**, *62*, 1501.
(21) Park, S. Y.; Lee, C. H.; Song, W. J.; Seoul, C. *Curr. Appl. Phys.* **2001**, *1*, 116.
(22) Yoshimura, D.; Tokoyama, T.; Ito, E.; Ishii, H.; Ouchi, Y.; Hasegawa, S.; Seki, K. *Synth. Met.* **1999**, *102*, 1145.
(23) Ganzorig, C.; Fujihira, M. *Appl. Phys. Lett.* **2002**, *81*, 3137.
(24) McCarthy, B.; Coleman, J. N.; Czerw, R.; Dalton, A. B.; Panhuis, M.; Maiti, A.; Drury, A.; Bernier, P.; Nagy, J. B.; Lahr, B.; Byrne, H. J.; Carroll, D. L.; Blau, W. J. *J. Phys. Chem. B* **2002**, *106*, 2210.